



Clinical and pathological effects of intrathecal injection of mesenchymal stem cell-derived neural progenitors in an experimental model of multiple sclerosis

Violaine K. Harris, Qi Jiang Yan, Tamara Vyshkina, Sadia Sahabi, Xinhe Liu, Saud A. Sadiq*

Multiple Sclerosis Research Center of New York, 521W, 57th St., 4th floor, New York, NY, 10019, United States

ARTICLE INFO

Article history:

Received 28 April 2011

Received in revised form 27 July 2011

Accepted 26 August 2011

Available online xxxx

Keywords:

Multiple sclerosis

Neural stem cells

EAE

Bone marrow stem cells

Demyelination

Intrathecal therapy

Nestin

ABSTRACT

Multiple sclerosis (MS) is associated with irreversible disability in a significant proportion of patients. At present, there is no treatment to halt or reverse the progression of established disability. In an effort to develop cell therapy-based strategies for progressive MS, we investigated the pre-clinical efficacy of bone marrow mesenchymal stem cell-derived neural progenitors (MSC-NPs) as an autologous source of stem cells. MSC-NPs consist of a subpopulation of bone marrow MSCs with neural progenitor and immunoregulatory properties, and a reduced capacity for mesodermal differentiation, suggesting that this cell population may be appropriate for clinical application in the CNS. We investigated whether MSC-NPs could promote repair and recovery after intrathecal injection into mice with EAE. Multiple injections of MSC-NPs starting at the onset of the chronic phase of disease improved neurological function compared to controls, whereas a single injection had no effect on disease scores. Intrathecal injection of MSC-NPs correlated with reduced immune cell infiltration, reduced area of demyelination, and increased number of endogenous nestin-positive progenitor cells in EAE mice. These observations suggest that MSC-NPs may influence the rate of repair through effects on endogenous progenitors in the spinal cord. This study supports the use of autologous MSC-NPs in MS patients as a means of promoting CNS repair.

© 2011 Elsevier B.V. All rights reserved.

1. Introduction

Multiple sclerosis (MS) is a demyelinating disease that is characterized pathologically by widespread discrete inflammatory lesions within the brain and spinal cord parenchyma. Over a variable period of time the accumulating lesion burden results in a progressive clinical course that is associated with physical or cognitive disability [1]. While the mechanisms underlying disease progression remain unclear, it is likely that endogenous repair mechanisms are inhibited by the hostile lesion environment caused by chronic disease inflammation, leading to remyelination failure, axonal loss, and long-term disability. There is a dire need to develop therapeutic strategies aimed at prevention or reversal of progression-related disability through remyelinating and/or neuroprotective mechanisms.

Stem cell biology and its clinical application represent an exciting area of investigation that has the potential of having therapeutic efficacy for progressive forms of MS and other neurodegenerative

diseases. If a cell therapy-based approach is to be translated into clinical trials, a number of preclinical studies are necessary in order to identify the source of cells (adult or embryonic), the optimal route of administration, dosing regimen, and long term safety, tolerability and efficacy. In addition, specifically in MS, the multiplicity of lesions in the brain and spinal cord require that any therapeutic strategy would result in widespread dissemination of the transplanted cells within the CNS. Because MS is an autoimmune condition, any factors that contribute to host immune activation such as tissue rejection of transplanted cells, have the added risk of exacerbating the disease activity. One strategy to circumvent immune rejection is to use an autologous source of cells, such as bone marrow mesenchymal stem cell-derived neural progenitors (MSC-NPs). Delivery of these cells to the multiple areas of involvement may be best possible by exploiting the cerebrospinal fluid flow dynamics to enable transport of these cells to both the brain and spinal cord.

MSC-NPs have been characterized as a subset of MSCs that exhibit neuroectodermal lineage characteristics including neurosphere morphology, clonogenic growth, and expression of neural markers [2,3]. We sought to investigate whether MSC-NPs could promote remyelination and recovery in the experimental autoimmune encephalomyelitis (EAE) mouse model of MS. MSC-NPs were injected intrathecally into EAE mice with chronic disability. We report that multiple injections of MSC-NPs improve clinical and pathological parameters of EAE, and are associated with promotion of endogenous repair mechanisms.

Abbreviations: MSC-NP, mesenchymal stem cell-derived neural progenitor; EAE, experimental autoimmune encephalomyelitis; CNS, central nervous system; CSF, cerebrospinal fluid; NFM, neurofilament medium; GFAP, glial acidic fibrillary protein; CDS, cumulative disease score; DPL, days post immunization.

* Corresponding author at: Multiple Sclerosis Research Center of New York, 521 West 57th St., New York, NY 10019, United States. Tel.: +1 212 265 8070; fax: +1 212 265 8194.

E-mail address: ssadiq@msrcny.org (S.A. Sadiq).

0022-510X/\$ – see front matter © 2011 Elsevier B.V. All rights reserved.

doi:10.1016/j.jns.2011.08.036

Please cite this article as: Harris VK, et al. Clinical and pathological effects of intrathecal injection of mesenchymal stem cell-derived neural progenitors in an experimental model of multiple sclerosis, *J Neurol Sci* (2011), doi:10.1016/j.jns.2011.08.036

2. Methods

2.1. Cell culture

Syngeneic mouse MSCs were derived from 9 week old C57BL/6 mice according to published protocols [4]. Briefly, femurs and tibias were dissected and flushed with 2% FBS in PBS. Bone marrow cells were washed and plated in MSC expansion medium (Mouse Mesencult® Proliferation medium, Stem Cell Technologies, Inc.) at a density of 1×10^6 cells/cm². Nonadherent hematopoietic cells were eliminated by complete media change every 3–4 days. When cells reached 70% confluency (approximately 3 weeks) cells were passaged with 0.25% trypsin for up to 20 passages. MSCs at passage 8 were free of hematopoietic cell contamination (CD45⁺/CD11b⁺) thus no further purification was needed. Mouse MSCs used for experimentation were between passage 8 and 17.

For MSC-derived neural progenitors (MSC-NPs), MSCs were cultured in low-adherence flasks in serum-free neural progenitor maintenance media (NPM, Lonza) containing NSF-1 (1×), and 20 ng/ml each of epidermal growth factor (EGF) and basic fibroblast growth factor (bFGF) for 21 days with complete media change every 2–3 days. Floating “neurospheres” were visible after 2 days. Single cell suspensions of MSC-NPs were obtained by centrifugation at 200×g for 5 min, resuspension in 1 ml room temperature TrypLE, and trituration 20 times with a sterile fire-polished glass pipette. MSC-NPs were then washed twice in PBS prior to each experiment. Trypan blue staining and hemacytometer counting were performed to confirm single cell suspension and >80% viability. For *in vivo* tracking of injected cells, mouse MSCs were labeled with 800 nM CellTracker™ CM-Dil (Invitrogen) according to manufacturer's instructions just prior to induction of MSC-NPs.

2.2. Flow cytometry

Cells were resuspended in staining buffer (2% FBS/PBS) and cell surface staining was carried out using FITC-conjugated rat anti-mouse CD45, FITC-conjugated rat anti-mouse Sca-1, or with unconjugated rat anti-mouse CD9 or CD44 (all primary antibodies 1:100, BD Pharmingen) followed by Alexa 488-conjugated goat anti-rat secondary antibody (1:2500, Molecular Probes). For intracellular NF-M staining, cells were resuspended in BD Cytofix/Cytoperm™ fixation and permeabilization solution then washed with BD Perm/Wash buffer according to manufacturer's instructions. Cells were incubated with rabbit anti-Neurofilament-M 1:1000 (Chemicon) followed by Alexa 488-conjugated goat anti-rabbit secondary antibody (1:2500, Molecular Probes). Analysis was performed on a FACS Aria flow cytometer (BD).

2.3. Quantitative real-time PCR (qPCR)

Total RNA was extracted from MSC and MSC-NP paired samples using QIAGEN RNeasy Plus, and first-strand cDNA was synthesized from equal amounts of RNA from each sample using Superscript III (Invitrogen). mRNA expression was measured by qPCR using TaqMan® Gene Expression Assays (Applied Biosystems, Inc) for Sca1 (Ly6a) (Mm00726565_s1), smooth muscle isoform of α 2-actin (SMA) (Mm01546133_m1), Nestin (Mm00450205_m1), medium neurofilament (NF-M) (Mm00456201_m1), and glial acidic fibrillary protein (GFAP) (Mm01253034_m1). All target genes were normalized to Hprt1 (Mm00446968_m1) endogenous control. QPCR was carried out with TaqMan® Fast Universal PCR Master Mix (Applied Biosystems) in a 96 well format using 7900HT Fast Real-Time PCR System. Relative quantification was analyzed using RQ software (Applied Biosystems).

2.4. Adipogenic and osteogenic differentiation

MSCs or MSC-NPs were plated at 2500 cells/cm² in MSC expansion medium and differentiation was induced after 48 h. All treatment

conditions were assessed in duplicate. For adipogenic differentiation, adipogenic induction media (DMEM containing 2% FBS, 1 μ M dexamethasone, 0.5 mM IBMX, 5 μ g/ml insulin, 50 μ M indomethacin, 100 U/ml penicillin, and 100 μ g/ml streptomycin) was added for 14 days with media change every 2–3 days. Controls were maintained in MSC expansion medium only. To visualize lipid accumulation, cultures were fixed in 4% paraformaldehyde for 30 min and stained with 0.3% Oil Red O in 60% isopropanol for 50 min and counterstained with hematoxylin. Red staining was visualized by light microscopy.

For osteogenic differentiation, cells were plated as above and cultured in osteogenic induction medium (DMEM containing 2% FBS, 1.0 μ M dexamethasone, 50 μ M ascorbic acid, 10 mM glycerol 2-phosphate, 100 U/ml penicillin, and 100 μ g/ml streptomycin) for 14 days with media change every 2–3 days. Controls contained MSC expansion media alone. Cells were fixed in 70% cold ethanol for 1 h and stained with 1% Alizarin Red S (Millipore) for 30 min. Red staining was visualized by microscopy.

2.5. Co-culture assays

Mouse MSCs or MSC-NPs were plated 15,000 cells/cm² one day prior to T cell isolation. CD4⁺/CD25[−] T cells were isolated from C57BL/6 mouse splenocytes using untouched CD4⁺ T cell isolation kit (Miltenyi) followed by CD25 microbead kit (Miltenyi) to deplete activated T cells. CD4⁺/CD25[−] cells were labeled with 2.5 μ M CFSE and plated at a 10:1 ratio with MSCs or MSC-NPs in RPMI media with 10% FBS. Cells were left unstimulated, or were stimulated with anti-CD3/CD28 Dynabeads (Invitrogen). All conditions were tested in duplicate. After 72 h, T cells were collected, stained with anti-mouse CD4-Pacific Blue (BD), and analyzed for CFSE staining by flow cytometry with a BD FACS Aria. Population doublings were analyzed using DeNovo FCS Express V3 software.

2.6. EAE induction and MSC-NP injections

All animal experiments were approved by the St. Luke's Roosevelt Hospital Center IACUC. 8 week old female C57BL/6 mice purchased from Jackson Laboratory (Bar Harbor, ME) were immunized subcutaneously with 200 μ g of the myelin oligodendrocyte glycoprotein peptide 35–55 (MOG_{35–55}; AnaSpec, Fremont, CA) diluted in 100 μ l PBS and prepared in an equal volume of complete Freund's adjuvant containing 5 mg/ml *Mycobacterium tuberculosis* (H37Ra) (Difco, Detroit, MI). Mice received i.v. injection of 200 ng pertussis toxin (List Biological Laboratories, Campbell, CA) on days 0 and 2 post immunization (p.i.).

Mice were weighed and evaluated for neurological disability daily. Disability was scored using a 0–13 EAE scale [5] which was modified from the standard 0–5 scale [6]. The 0–13 scale was preferred over the traditional 0–5 scale because in our preliminary pilot studies the modified scale correlated better with the clinical neurological examination of the mice. The modified scoring system represents the sum of the tail and all four limbs and thus allows for more robust assessment of clinical effects during chronic EAE. In the modified 0–13 scale, the tail and limbs were scored individually as follows. The tail was scored as 0 (normal tail), 1 (mild tail weakness), 2 (severe tail weakness), or 3 (completely paralyzed tail). Each hind-limb was scored separately as 0 (normal hind limb strength), 1 (mild weakness), 2 (moderate weakness), 3 (severe weakness), or 4 (full paralysis). Fore limbs were scored together as 0 (normal movement), 1 (weakness and difficulty using forelimbs to pull body), or 2 (paralysis). The scores were tabulated for a final score up to 13. The scorer was blinded to the treatment groups. Scores based on the traditional 0–5 scale were also determined for comparison.

Mice that had developed EAE by day 21 were divided into 6 treatment groups that received three intrathecal injections on days 21, 28, and 35 post immunization. Groups were as follows: Group 1, PBS ($n = 18$); Group 2, 2×10^6 MSC-NPs each injection ($n = 18$); Group

3.5×10^4 MSC-NPs each injection ($n = 16$); Group 4, 2×10^5 MSC-NPs each injection ($n = 18$); Group 5, 1×10^6 MSC-NPs each injection ($n = 14$) and Group 6, 1×10^6 MSC-NPs in first injection on day 21 followed by two injections of PBS on days 28 and 35 ($n = 18$). Stem cells were delivered intrathecally via the cisterna magna according to published protocols [7,8]. Briefly, mice were anesthetized and fixed on a stereotaxic apparatus with the incisor tilt positioned at -8° such that the site of injection, the cisterna magna, was nearly the highest point of the animal. A 1 cc syringe (25 gauge) with permanently attached needle was inserted along the horizontal line into the top of the foramen magnum. A volume of 20 μ l of resuspended cells in PBS or PBS alone was injected slowly, followed by a 2 minute period before the needle was withdrawn. A drop of PBS (100 μ l) was placed on top of the injection site in order to reduce cell leakage.

Average daily scores, pre-treatment scores (disease onset to day 21), and post-treatment scores (day 22 to termination) were calculated for each group. Cumulative disease score (CDS) was calculated as the sum of all scores between days 1 and 21 (pre-treatment) and days 22 and 87 (post-treatment). Day 87 was the last day for which all animals in every group were scored, and was thus chosen as the endpoint for calculating CDS.

2.7. Immunohistochemistry

Mice were sacrificed on days 37, 56, and 91 post-immunization, corresponding to 2.3 weeks, 5 weeks and 10 weeks after the first stem cell injection. The day 37 timepoint was designed to correspond to 48 h post third injection for the multiple injection group. 5 mice per group per time point were removed for histology, representing the average clinical score of their group. Mice were terminally anesthetized with an intraperitoneal injection of pentobarbital 40 mg/kg and perfused through the left ventricle with saline followed by 10% formalin and post-fixation for 24 h. Following fixation, the brain and spinal cord were cut into 0.5 cm blocks and paraffin embedded. 5 μ m transverse spinal cord sections were analyzed by immunohistochemical staining using the following antibodies: anti-CD3 (M-20; Santa Cruz) (1:100), anti-MBP (C-16; Santa Cruz) (1:500), anti-Nestin (Millipore) (1:100), and anti-GFAP (Dako) (1:500). Primary antibodies were detected with either anti-goat or anti-mouse secondary antibody (1:1000) conjugated with Alexa 488 (Invitrogen). 4', 6-diamidino-2-phenylindole (DAPI; Invitrogen) was used for cell nuclei detection. Negative control samples were performed omitting the primary antibody.

Quantification of immune cell infiltration, demyelination, and Nestin staining was performed on at least five spinal cord cross-sections per animal spanning the length of the spinal cord. All quantitation was performed in a blinded manner by omission of red (DiI) fluorescence. Immunohistochemistry was performed with anti-CD3 as described above. The number of cells positive for CD3 were counted manually for all positive fields (average of 6 fields per spinal cord) and divided by the area of the field. Quantitation of DAPI positive cells was performed using ImageJ software. Digital images of were captured at 40 \times magnification with a Zeiss LSM 510 META confocal microscope. Area of demyelination was quantified on composite 10 \times digital images of MBP-stained spinal cords assembled using tile scan. Areas of demyelination were identified on individual tiled images according a modified protocol [9]. Briefly, the area of each spinal cord section and the area of grey matter were traced and measured using the overlay Closed Bezier tool in Zen 2009 software. White matter area was determined by subtracting grey matter area from whole spinal cord area. Area of white matter demyelination was determined using standard morphological criteria with evidence of decreased MBP intensity relative to the adjacent white matter, and measured as above. Demyelination for each mouse was expressed as a percentage of the total white matter area sampled. Areas of demyelination were confirmed by luxol fast blue staining of an adjacent section. For Nestin quantitation, endogenous

Nestin expression was determined by immunohistochemistry and visualized by confocal microscopy at 20 \times . The number of discrete fields containing Nestin positive cells was counted manually.

2.8. Statistical analysis

Average EAE scores were analyzed by Kruskal-Wallis to test differences between all dose groups, and Mann Whitney to determine significance between individual treatment groups and control. For statistical analysis of CDS, only mice that had follow-up of at least 87 days were included. Cumulative scores from day 1 to 21 (baseline) were compared by ANOVA. Cumulative scores from day 22 to 87 for each group were log transformed and differences were assessed using multiple linear regression adjusted for baseline (log) CDS, and day of disease onset. All other data were analyzed by one way ANOVA to test differences between multiple groups, and unpaired, two-tailed, Student's *t*-test to determine significance between two groups. Statistical significance was set to *p* values < 0.05. SAS v9.2 and GraphPad Prism 4 were used to calculate significance.

3. Results

3.1. Characterization of MSC-NP cell population

In order to establish pre-clinical proof-of-concept efficacy studies supporting the use of autologous MSC-derived neural progenitors for the treatment of MS, we first derived and characterized the homologous cell population from mice. MSCs derived from bone marrow from C57Bl/6 mice displayed adherent MSC morphology (Fig. 1A) and characteristic CD9⁺/CD44⁺/Sca1⁺/CD45⁻ cell surface phenotype (Fig. 1D). The neuroectodermal conversion of MSCs into MSC-derived neural progenitors (MSC-NP) has been described previously for human MSCs [2]. We used a similar protocol to derive MSC-NPs from mouse MSCs. Mouse MSC-NPs displayed characteristic "neurosphere" morphology with clusters of cells growing in suspension (Fig. 1B). We confirmed the neural lineage potential of MSC-NPs by gene expression analysis of genes associated with neural lineage differentiation including Nestin (neural stem cell marker), medium neurofilament (NFM, neuronal marker), and GFAP (glial and neural stem cell marker). Nestin and GFAP were upregulated approximately 2-fold, and NFM was upregulated > 100 fold (Fig. 1F). Protein expression of Nestin and GFAP was detectable at low levels by immunocytochemistry (data not shown) and significant NFM protein was detectable by both immunocytochemistry (data not shown) and flow cytometry (Fig. 1E) in MSC-NPs. Conversely, MSC-NPs expressed decreased mRNA levels of the MSC marker smooth muscle isoform of alpha actin (SMA), as well as a slight decrease in Sca1 and (Fig. 1F) which was consistent with reduced cell surface expression of MSC markers CD9, CD44, and Sca1 (Fig. 1E) in MSC-NPs compared to MSCs. Expression of CD45 in MSC-NPs remained absent (data not shown).

A defining characteristic of multipotential MSCs is their ability to undergo *in vitro* differentiation into adipocytes and osteocytes [10]. To test whether MSC-NPs are also capable of differentiation into mesodermal lineages, MSC-NPs were cultured under adipogenic and osteogenic differentiation conditions. Mouse MSCs were capable of adipogenic and osteogenic differentiation *in vitro* (Fig. 2A and C). MSC-NPs showed markedly decreased Oil Red O⁺ lipid vacuole formation compared to MSCs after culture in adipogenic induction medium (Fig. 2B). Similarly, MSC-NPs displayed decreased alizarin red staining indicative of calcium deposition compared to MSCs after culture in osteogenic induction medium (Fig. 2D). Reduced mesodermal plasticity, together with the observed increase in neural marker expression and decreased MSC marker expression in the MSC-NP cell population indicate a conversion from multi-potent MSCs to a more lineage-restricted neural progenitor-like population.

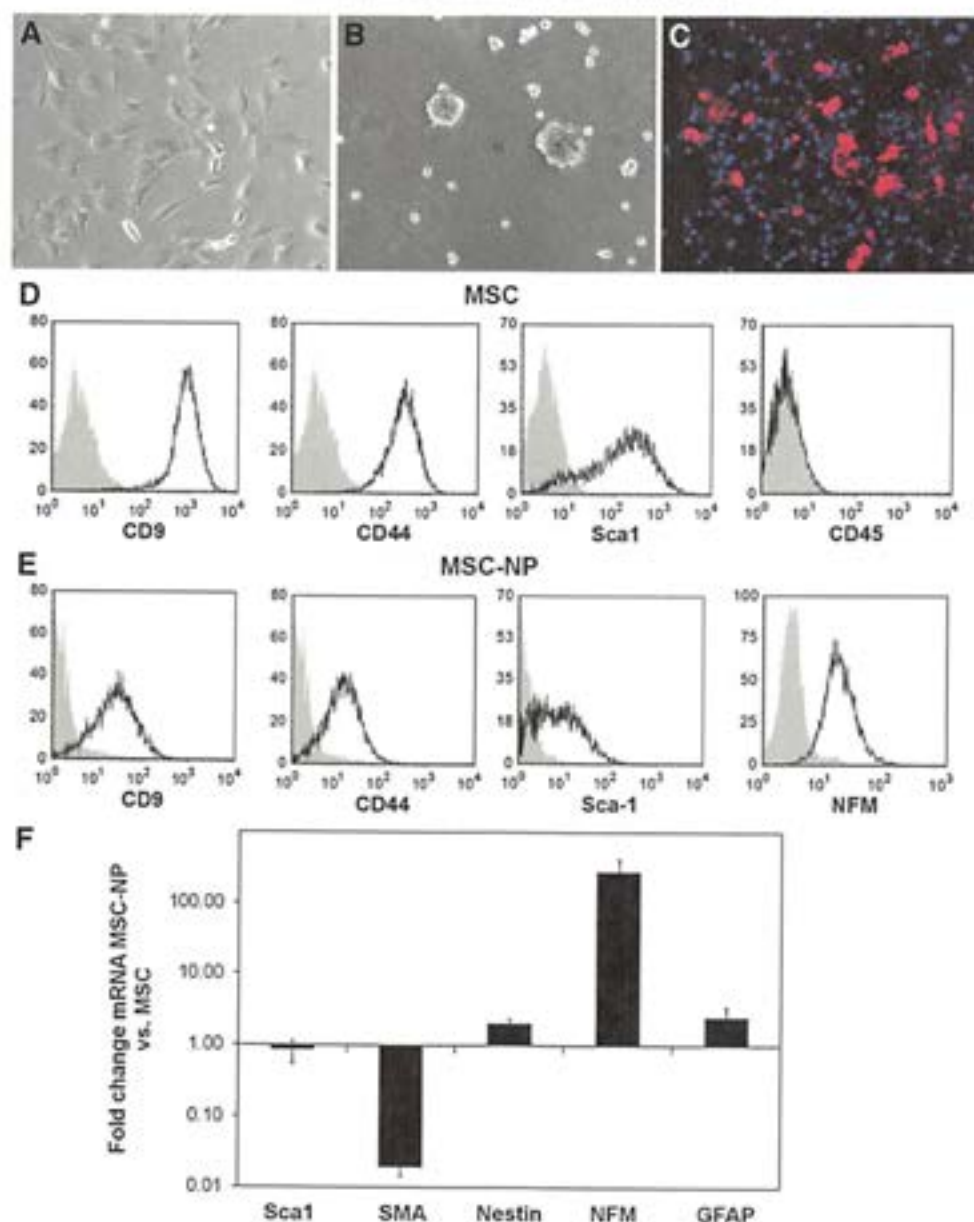


Fig. 1. Characterization of mouse MSC and MSC-NP cell populations. (A) Morphology of mouse MSCs at passage 8 ($10\times$ magnification). (B) "Neurosphere" morphology of MSC-NPs ($10\times$ magnification). (C) Red fluorescence of DiI labeled MSC-NPs analyzed prior to injection into mice. (D, E) Cell surface phenotype of MSCs (D) and MSC-NPs (E) determined by flow cytometry using antibodies against CD9, CD44, Sca1, and CD45 (represented by black histograms) compared to isotype controls (grey filled histograms). Intracellular Neurofilament-M (NFM) staining was also evaluated in MSC-NPs in (E). (F) Gene expression analysis by qPCR of MSC-NPs compared to the MSCs from which they were derived. MSC-NPs showed increased mRNA expression of neural markers Nestin, NFM, and GFAP, and decreased expression of MSC markers Sca1 and SMA. Values represent mean of 4 separate experiments. Error bars represent SE.

3.2. Immunoregulatory properties of MSC-NPs

MSCs possess an array of immunoregulatory properties which include suppression of T cell activation and proliferation [11]. To investigate whether MSC-NPs retain the immunomodulatory properties of MSCs, we incubated MSCs or MSC-NPs together with anti-CD3/CD28-stimulated T cells from syngeneic mouse splenocytes at a ratio previously shown to suppress T cell proliferation [11]. Co-culture with either MSCs or MSC-NPs reduced proliferation of CD4⁺T cells (Fig. 3A–D). Only 3.5% and 6.3% CD4⁺T cells underwent 5 or more population doublings when co-cultured with MSCs or MSC-NPs, respectively, compared with 24.8% of CD4⁺T cells without co-culture (Fig. 3E). These results suggest that MSC-NPs display immunomodulatory

activity that is similar *in vitro* to the known properties of unmanipulated MSCs.

3.3. Injection of mouse MSC-NPs improves neurological disability in EAE mice

To determine whether MSC-NPs affect CNS repair and remyelination, we injected syngeneic mouse MSC-NPs intrathecally into mice with EAE. EAE was induced upon immunization of mice with an antigenic peptide of the myelin oligodendrocyte glycoprotein (MOG) and showed characteristic monophasic acute inflammatory phase with average onset 12 days post-immunization (DPI) (Table 1). MSC-NP injections commenced at the onset of the chronic phase on day 21

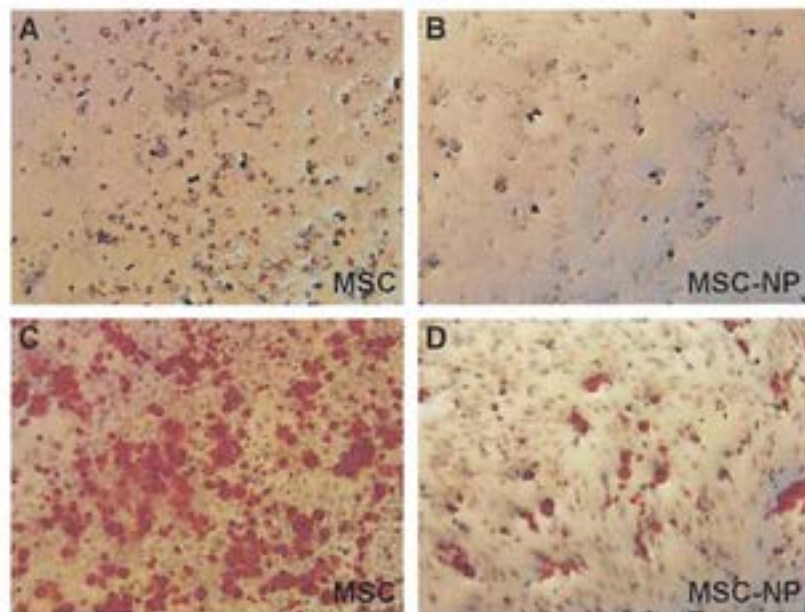


Fig. 2. Loss of mesodermal differentiation capacity in MSC-NPs. (A,B) Oil Red O staining of accumulated lipids after adipogenic differentiation demonstrating limited adipogenic differentiation by MSC-NPs (B) compared to MSCs (A). (C,D) Alizarin Red staining of calcium deposition after osteogenic differentiation demonstrating limited osteogenic differentiation by MSC-NPs (D) compared to MSCs (C). Data is representative of two separate experiments.

in order to better model therapy aimed at patients with established MS. Cells were injected intrathecally (via cisterna magna) in mice as a means to disseminate cells throughout the brain and spinal cord.

Mouse MSC-NPs were labeled with a red fluorescent dye (DiI) for tracking (Fig. 1C), and resuspended in phosphate buffered saline (PBS) and compared to PBS only injections (Group 1). Dosing of MSC-NPs ranged from 2×10^4 to 1×10^6 cells in each of three injections given days 21, 28, and 35 (Groups 2 through 5). A single injection of 1×10^6 cells on day 21 was also included (Group 6). Prior to treatment, there were no significant differences in disease onset, maximum EAE score, average EAE score, or cumulative disease score (CDS) over the first 21 days between any of the groups (Table 1 and Fig. 4B). MSC-NP or PBS-injected EAE mice were followed up to 10 weeks post-first injection. Following the monophasic acute phase, group 1 control mice displayed a chronically stable disease course (Fig. 4A). In contrast, mice receiving multiple injections of MSC-NPs demonstrated a dose responsive improvement in EAE scores over time, with greatest efficacy in the 2×10^5 cell dose group (group 4) (Fig. 4A). Group 2 and 3 mice receiving multiple injections of low dose MSC-NPs demonstrated significantly reduced average EAE score and cumulative disease score as a result of treatment (Table 1 and Fig. 4C). Multiple injections of 2×10^5 cells (group 4) resulted in highly significant improvement in average daily (Fig. 4A) and post-treatment (Table 1) EAE scores, as well as significant improvement in CDS 22–87 (Fig. 4C), compared to controls. Similar improvements were observed following multiple injections of the highest dose of 1×10^6 cells (group 5) (Table 1 and Fig. 4C). Significant improvement in outcomes was also noted using the traditional 0–5 scale to measure EAE (Supplemental Table 1 and Supplemental Fig. 1). These results show amelioration of neurological disability associated with multiple intrathecal MSC-NP injections, with 2×10^5 MSC-NP dose as the optimal dose in EAE mice.

Mice injected with a single dose of 1×10^6 MSC-NPs (Group 6) showed no difference in post-treatment CDS 22–87 compared to PBS controls (Fig. 4C). Similarly, there was no reduction in average post-treatment scores, which were actually increased compared to the control group (Table 1), probably due to the slightly higher

baseline average in group 6. Overall these data suggest that multiple dosing of intrathecally injected MSC-NPs compared to a single dose correlates with increased efficacy.

3.4. Reduced T cell infiltration and demyelination in MSC-NP-treated mice

Mice were sacrificed for post-mortem analysis (approximately 5 mice/group/timepoint) at 2.3, 5, and 10 weeks after the first MSC-NP injection. Gross examination of each mouse at each timepoint showed no adverse events associated with cell injections. Group 1 (control), groups 4 and 5 (multiple high doses) and group 6 (single high dose) were examined further for histopathology. We found evidence of engraftment of injected DiI-labeled MSC-NPs at all timepoints (Fig. 5C and D). MSC-NPs were found in inflammatory foci in parenchyma of the brain stem (data not shown) and spinal cord (Fig. 5A–D) as defined by areas of T-cell infiltration ($CD3^+$, labeled green). We observed that the presence of engrafted MSC-NPs in lesions correlated with decreased $CD3^+$ T cell staining (Fig. 5C and D). Quantitation of $CD3^+$ cells over the length of the spinal cord demonstrated that MSC-NP treated mice had reduced T cell infiltration compared to controls, and these differences reached significance at the 10 week time point (Fig. 5E). Specifically, mice injected either once or three times with the highest dose of 1×10^6 MSC-NPs demonstrated significantly reduced T cell infiltration (Fig. 5E). There were no differences in total number of DAPI+ cells in sections between any of the groups (Supplemental Table 2).

We next analyzed spinal cord demyelination in order to assess the effect of injected MSC-NPs on degree of demyelination. Myelin was stained with anti-MBP antibody, and the area of white matter demyelination was calculated for each section from PBS (Fig. 6A) and MSC-NP (Fig. 6B) treated EAE mice. We observed significantly reduced area of white matter demyelination in EAE mice treated with three doses of 2×10^5 or 1×10^6 MSC-NPs compared to PBS controls when examined 5 and 10 weeks after the first injection of MSC-NPs (Fig. 6C). EAE mice receiving a single dose of 1×10^6 MSC-NPs also had reduced area of demyelination which was only significant at the 10 week

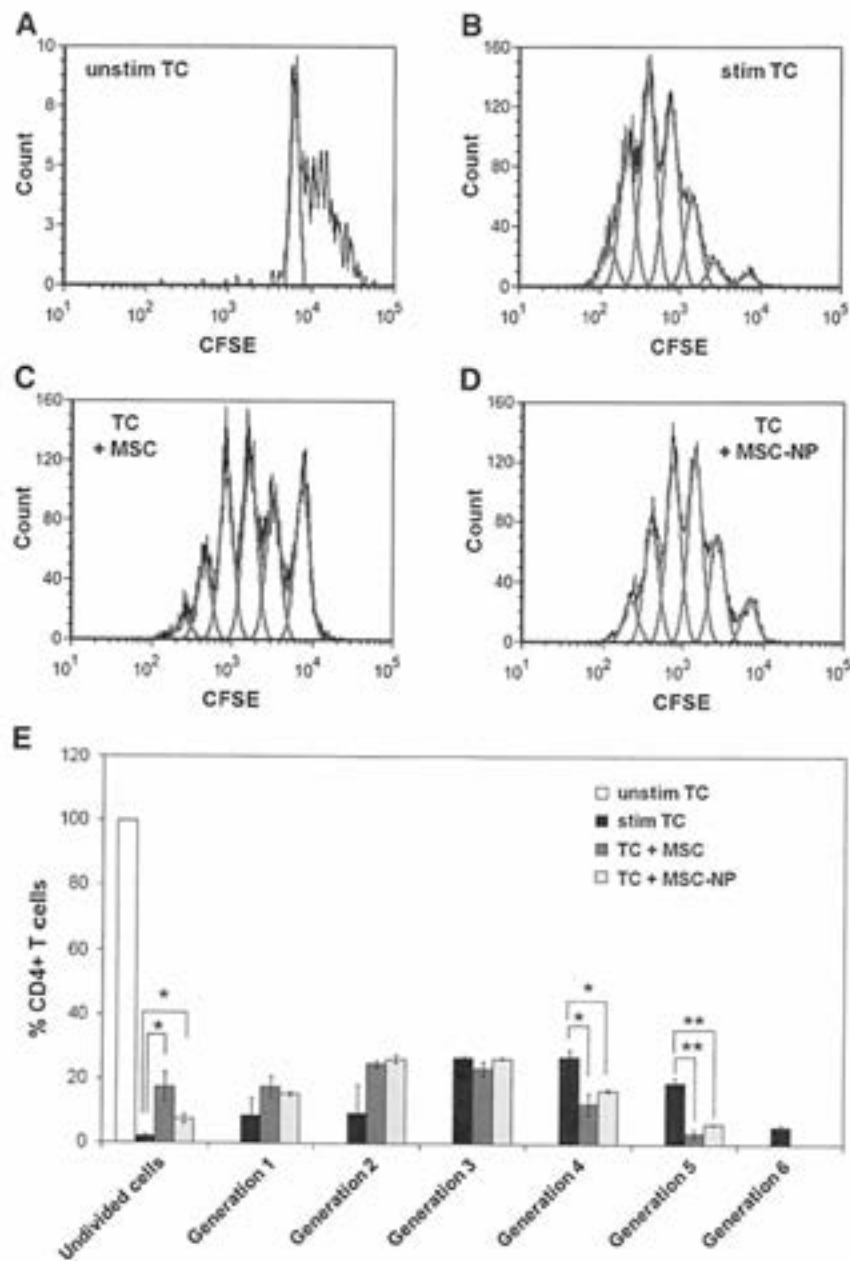


Fig. 3. Suppression of T cell proliferation by MSCs and MSC-NPs. CFSE-labeled naive CD4⁺/CD25⁻ T cells were either unstimulated (A), or stimulated with anti-CD3/CD28 for 3 days either alone (B) or co-cultured with syngeneic MSCs (C) or MSC-NPs (D) at a 10:1 ratio. Representative histograms are shown with population analysis in grey. (E) Population doublings expressed as percentage of CD4⁺ cells. Values represent mean \pm SD. *, $p < 0.05$; **, $p < 0.01$. Representative experiment is shown.

Table 1

Disability assessment for each treatment group.

Treatment groups	Treatment regimen	Disease onset, DPI	Maximum EAE score pre-treatment ^a	Average EAE score pre-treatment ^a	Average EAE score post-treatment ^b
Group 1	PBS	12.1 \pm 1.8	11.1 \pm 1.4	8.2 \pm 2.0	7.5 \pm 2.0
Group 2	2 \times 10 ⁴ MSC-NP multiple dose	12.1 \pm 1.2	10.1 \pm 2.2	7.5 \pm 2.3	5.9 \pm 1.91
Group 3	5 \times 10 ⁴ MSC-NP multiple dose	11.7 \pm 1.6	10.0 \pm 2.0	7.5 \pm 2.1	5.6 \pm 2.51
Group 4	2 \times 10 ⁵ MSC-NP multiple dose	11.4 \pm 1.0	11.0 \pm 1.5	8.1 \pm 2.0	5.4 \pm 1.61
Group 5	1 \times 10 ⁶ MSC-NP multiple dose	12.3 \pm 2.0	10.2 \pm 1.9	7.5 \pm 2.3	5.4 \pm 1.61
Group 6	1 \times 10 ⁶ MSC-NP single dose	12.4 \pm 1.9	11.6 \pm 1.6	9.1 \pm 1.9	8.9 \pm 2.41

Values represent mean \pm SD.

^a Calculated from disease onset to day 21.

^b Calculated from day 22 to termination.

† $p < 0.05$, †† $p < 0.01$; compared to group 1.

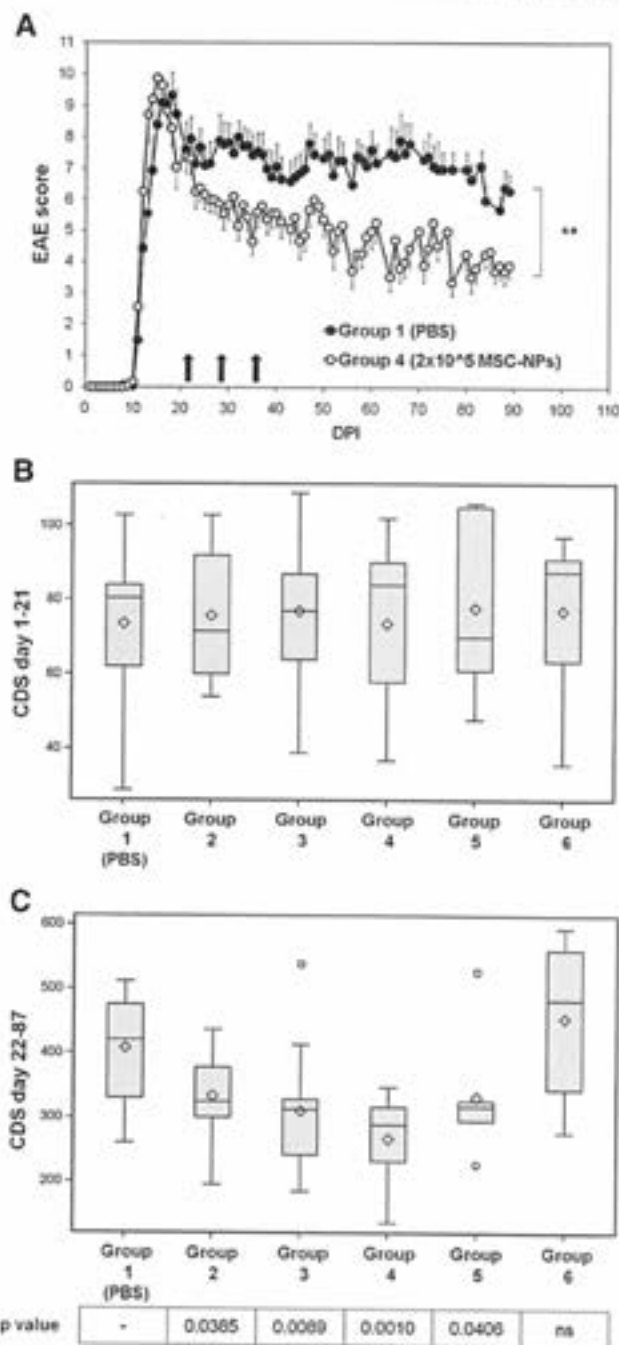


Fig. 4. Multiple intrathecal MSC-NP injections improve EAE disease course and cumulative disease. (A) Daily average EAE scores of mice treated with three intrathecal doses ($3 \times$) of PBS (black circles) or with 2×10^5 MSC-NPs (open circles). Arrows indicate time of injection. Error bars represent SE. From day 45 onwards, the average daily scores for group 4 were statistically significant ($p < 0.01$) from group 1 as determined by Mann Whitney. (B,C) Boxplots showing pre-treatment CDS between days 1 and 21 (B), and post-treatment CDS between days 22 and 87 (C). Treatment groups included the following: Group 1 (PBS $3 \times$), Group 2 (2×10^4 MSC-NPs $3 \times$), Group 3 (5×10^5 MSC-NPs $3 \times$), Group 4 (2×10^5 MSC-NPs $3 \times$), Group 5 (1×10^6 MSC-NPs $3 \times$), and Group 6 (1×10^6 MSC-NPs $1 \times$). *, $p < 0.05$; **, $p < 0.01$; ***, $p < 0.001$; ns = not significant.

timepoint. Although reduced demyelinated area did not completely correlate with cell dose or number of injections, the two multiple dose groups that showed the smallest cumulative area of demyelination, also showed significant amelioration of EAE severity.

3.5. Increased endogenous neural progenitors associated with transplanted MSC-NPs

To investigate whether transplanted MSC-NPs had an effect on endogenous repair mechanisms, we analyzed nestin immunoreactivity as a marker for endogenous neural and astroglial progenitor cells. Nestin expression has been found to increase in response to pathological insult to the brain and spinal cord [12,13] and the re-expression of nestin in reactive astrocytes has been associated with neuroprotection [14]. In spinal cord sections of EAE mice, we found discrete regions of nestin-positive cells associated with some lesion areas at all timepoints in both control (Fig. 7A-C) and MSC-NP-injected (Fig. 7E-G) mice. In MSC-NP-treated mice, Dil positive MSC-NPs were frequently located in or around the nestin positive areas (Fig. 7E-G). We also examined GFAP expression as a marker of astrogliosis. In contrast to nestin, which was expressed in a minority of cells throughout the spinal cord, GFAP was highly expressed throughout all lesion areas at all timepoints (Fig. 7D and H). Dil⁺ MSC-NPs did not show detectable expression of Nestin or GFAP *in vivo*, consistent with low level of nestin and GFAP immunoreactivity in mouse MSC-NPs *in vitro*.

The number of discrete sites containing nestin positive cells was counted in the spinal cords in each treatment group. There was a significant increase in the number of nestin-positive sites in mice injected with three doses of MSC-NPs when examined at the 2.3 week (1×10^6 dose) or 5 week (both 2×10^5 and 1×10^6 doses) timepoints compared to PBS-injected controls (Fig. 7I). The slight increase in the number of nestin-positive sites after a single injection of MSC-NPs after 2.3 and 5 weeks was not significant compared to PBS controls. In all cases, the difference in number of nestin-positive sites between MSC-NP and PBS-injected mice was no longer apparent 10 weeks post injection (Fig. 7I). In contrast, there were no differences in GFAP staining between any of the groups (data not shown). These observations suggest that MSC-NPs may accelerate the rate of repair in EAE through effects on endogenous nestin-positive progenitors in the spinal cord.

4. Discussion

In the past two decades, the treatment of multiple sclerosis has radically changed with the introduction of disease modifying therapies (DMTs) that are able to effectively control the autoimmune/inflammatory components of the disease. While the relapse rates of patients have been dramatically reduced with the use of DMTs, it is unclear whether the underlying progression of the disease is halted by the use of these agents [15]. It is also recognized that DMTs are relatively ineffective in the treatment of progressive forms of MS [16]. To develop an effective treatment targeting progressive MS patients, a preclinical strategy aimed at controlling disease activity and inducing repair in an experimental model is necessary. A number of repair strategies are currently under preclinical investigation [17], although the positive results seen in animal models frequently do not extrapolate well to human trials. The most widely accepted model of MS is EAE, but in many instances disease amelioration and prevention is only possible if treatment is initiated at or near the onset of EAE symptoms [18]. The ability to block, delay, or reduce disability in EAE may not necessarily predict efficacy in MS due to our inability to intervene therapeutically in MS until well after disease onset. To overcome this problem, the current study was designed such that treatment was initiated in clinically established EAE to better mimic the complexity of the clinical situation and to best determine reversal of disease pathology.

MSC-NPs are derived with minimal manipulation from autologous MSCs, and thus are a convenient source of adult stem cells with neural progenitor properties for use in CNS repair strategies. The neural lineage potential of MSC-NPs, as evidenced by upregulation of neural-specific genes such as Nestin and Neurofilament M, is consistent with previous studies which demonstrated that the culture of MSCs under conditions

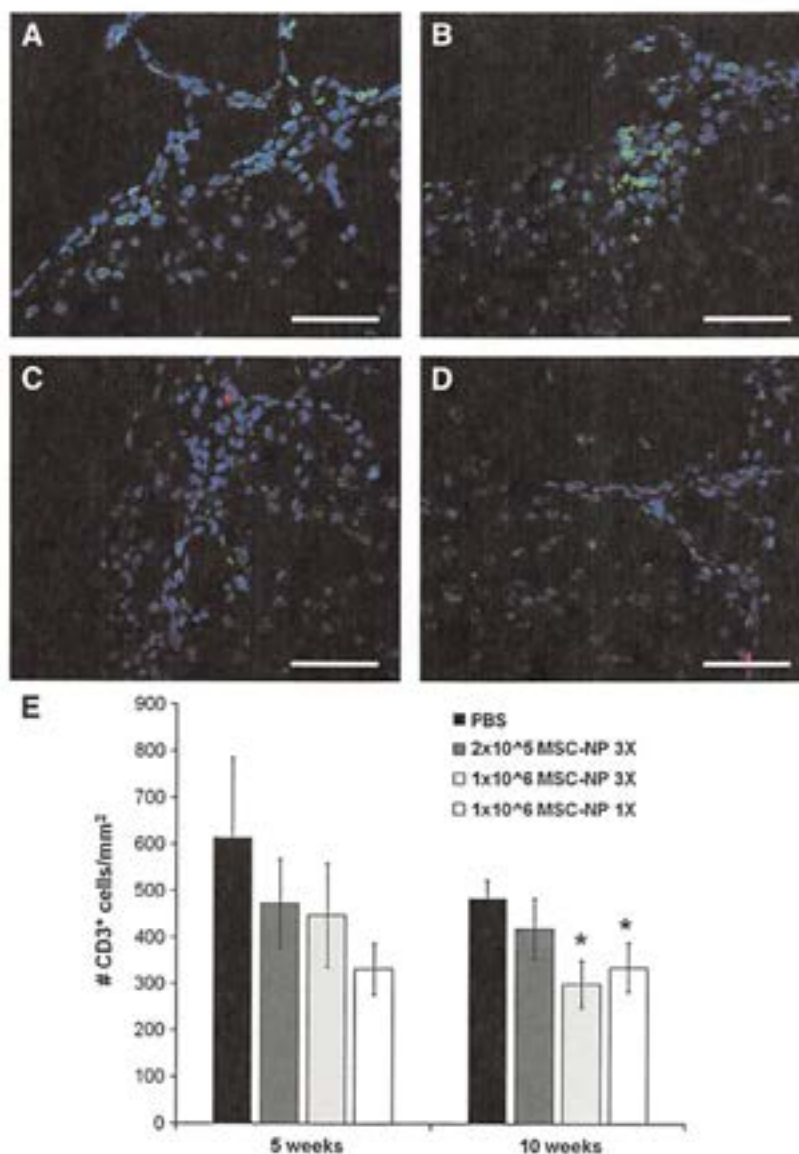


Fig. 5. Decreased T cell infiltration in MSC-NP-treated EAE mice. Mice were sacrificed 5 weeks (A and C), or 10 weeks (B and D) after the first injection of PBS (A and B), or MSC-NPs (C and D). T cell infiltration was determined by immunofluorescence with anti-CD3, transplanted MSC-NPs were detected by DiI red fluorescence, and nuclei detected by DAPI. All samples were visualized by confocal microscopy at 40 \times . Sections shown are representative of Group 1 (PBS) in panels A and B, and Group 6 (1×10^6 MSC-NPs $1 \times$) in panels C and D. Scale bar equivalent to 50 μ m. (E) Quantitation of CD3⁺ T cell infiltration in control and treatment groups examined 5 and 10 weeks post-first injection. Values represent mean \pm SE. *, $p < 0.05$.

optimal for brain derived neural stem cells selects a fraction of MSCs (anywhere from 6% to 60%) which exhibit neurosphere morphology [2,19]. In addition, MSC-NPs exhibited *in vitro* electrophysiological properties indicating functional neuronal differentiation [3,19]. Despite the *in vitro* neural differentiation potential of these cells, we found no evidence of *in vivo* transdifferentiation after transplantation in EAE. In addition to neural markers, a number of trophic factors are also upregulated in MSC-NPs compared to MSCs, which may promote CNS repair *in vivo* [20]. The contribution of such trophic factors to the efficacy of MSC-NPs is currently under investigation.

Inherent in the characteristic multipotentiality of MSCs is a certain degree of heterogeneity, where multiple phenotypes can be detected representing different levels of osteoblastic, chondrocytic, and adipocytic lineage commitment [21,22]. The relationship between differentiation plasticity and overall therapeutic efficacy of MSCs remains ill defined, although it is likely that such a correlation exists with respect to therapeutic efficacy for skeletal disorders, for example. For

non-homologous applications such as CNS transplantation, the possibility of uncontrolled mesodermal lineage differentiation by transplanted MSCs remains a potential risk [23]. Our study revealed that only a small fraction of MSC-NPs retain mesodermal differentiation potential compared to MSCs, which is consistent with the existence of a small subpopulation of MSC-NPs that harbor bipotential properties [19]. The reduced capacity for MSC-NPs to undergo adipogenic or osteogenic differentiation may decrease the hypothetical risk of ectopic differentiation into mesodermal tissue upon CNS transplantation.

One of the key aims of this study was to compare the preclinical efficacy of multiple dosing vs. single dosing of MSC-NPs. We demonstrated that three injections of MSC-NPs spaced one week apart resulted in significant amelioration of disease symptoms compared to a single injection. A multiple injection regimen for MSC-based therapies is further supported by a similar study where multiple intrathecal administration of MSCs prolonged survival in a transgenic mouse model of amyotrophic lateral sclerosis [24]. Why multiple dosing

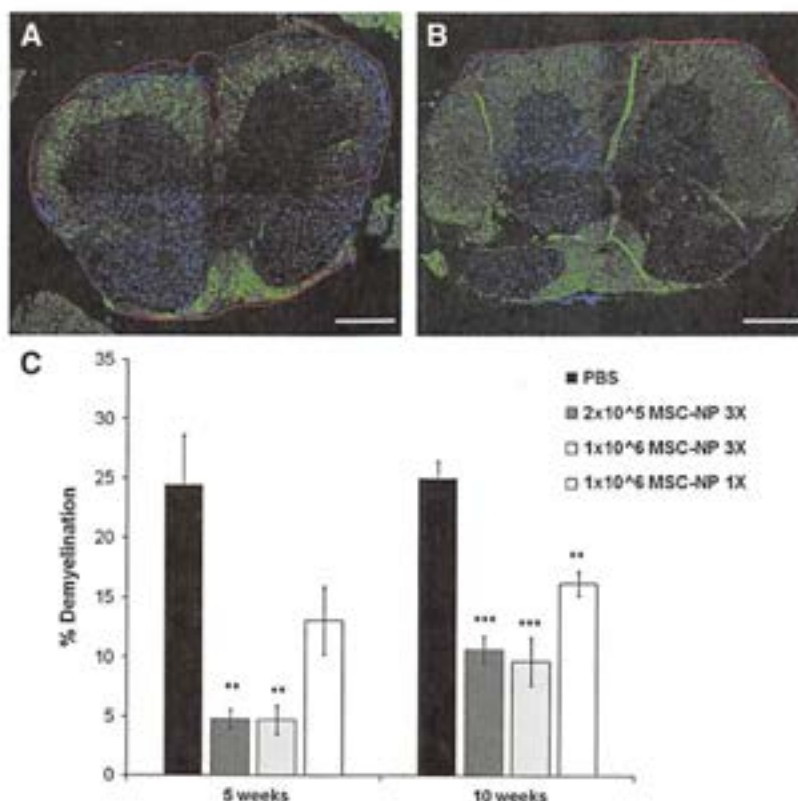


Fig. 6. Decreased area of demyelination in MSC-NP-treated EAE mice. Spinal cord demyelination was analyzed in sections from PBS (A) and MSC-NP (B) injected EAE mice by immunofluorescence with anti-MBP (green). Nuclei were detected by DAPI (blue) and visualized at 10 \times magnification. Sections shown are representative of Group 1 (PBS) in panel A, and Group 4 (2×10^5 MSC-NPs $3 \times$) in panel B analyzed 10 weeks post-first injection. Red line indicates demyelinated area. Scale bar equivalent to 200 μ m. (C) Quantitation of demyelinated area in the indicated treatment groups examined 5 and 10 weeks post-first injection. Values represent mean \pm SE. *, $p < 0.05$; **, $p < 0.01$; ***, $p < 0.001$.

and not a single dose results in neurological benefit is unclear, since in both cases we observed cell engraftment along with decreased immune cell infiltration. Cells were injected well after disease onset and thus any focal immunomodulatory effects of MSC-NPs may not be sufficient for disease recovery. Alternatively, it is possible that the clinical benefit seen with multiple dosing is not wholly dependent on immunomodulatory functions. Amelioration of EAE symptoms in the multiple injection groups correlated best with a sustained decrease in the area of demyelination and an early increase in the presence of nestin positive progenitors. These data suggest that sustained effects of MSC-NPs given in multiple doses may overcome a threshold level of demyelination resulting in clinical recovery. The exact mechanism(s) by which MSC-NPs exert clinical benefit requires further investigation, however the correlation with increased nestin-positive progenitors suggests a possible trophic effect. The potential trophic effects of circulating MSC-NPs may be short-lived in the CSF as cells die over time. Thus, repeated administration of cells would be required to sustain these effects.

Nestin-expressing multipotent progenitor cells in the adult CNS are increased in response to various types of injury [12–14,25], although the fate of nestin positive cells in the CNS and their exact contribution to repair remain unclear. Previous EAE studies have found nestin expression in astrocytes and ependymal cells in EAE lesions [26,27]. Nestin expression inactivated astrocytes may contribute to the neuroprotective function as a consequence of embryonic reversion of the mature glial cytoskeleton accompanied by expression of still unknown neuroprotective factors [14,28]. In our EAE study, the pattern of nestin expression only partially overlapped with GFAP expression, and, unlike nestin, there was no apparent correlation between MSC-NP injections and GFAP expression. Further investigation will be required in order

to elucidate the exact nature of nestin expressing cells during EAE and whether or not they represent a subpopulation of activated astrocytes. Nevertheless, our results that MSC-NP-injections correlate with increased areas with nestin expression suggest that the recruitment or induction of endogenous nestin expression may confer some kind of neuroprotection, possibly through a bystander mechanism mediated by MSC-NPs. These results suggest that one possible mechanism for the therapeutic efficacy of MSC-NPs is to increase the rate of CNS repair through the recruitment of nestin positive progenitor cells in the spinal cord in EAE.

In our approach, we selected the intrathecal route of administration as a means to deliver a significant number of cells to multifocal lesion areas in the CNS in order to better target repair mechanisms in a progressive MS patient population who is likely to be refractory to peripheral immunomodulatory agents. Previous studies which administered MSCs intravenously into EAE mice found only a small fraction of MSCs infiltrating into inflamed areas in the CNS, where they might directly influence repair mechanisms in the lesion [29–32]. In our study, we observed dissemination of MSC-NPs throughout the brain and spinal cord, where cells were primarily associated with the meninges near inflammatory foci, along with some migration into the parenchyma. We did not observe any cellular masses such as those recently reported following intracerebroventricular transplantation of MSCs [33]. Overall, the intrathecal application of MSC-NPs was well tolerated in mice with EAE. Similarly in humans with MS, previous clinical experience with intrathecal MSCs demonstrated that intrathecal administration is well tolerated at human dose equivalents to our EAE study [34–36].

Our preclinical studies using an experimental model of MS help establish the basis for future clinical studies using multiple doses of

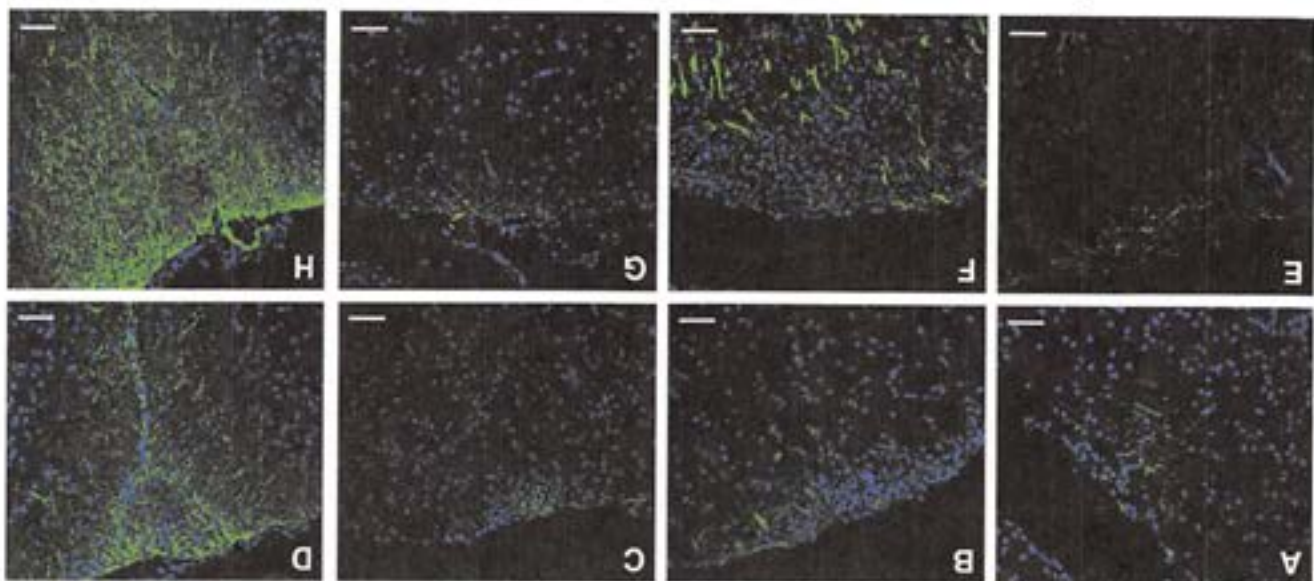


Fig. 7. Increased number of Nestin positive sites in spinal cord of hMSC-NP-treated EAE mice. Nestin expression was analyzed in CNS of EAE mice sacrificed 2.3 weeks (A and E), 5 weeks (B and F), or 10 weeks (C and G) after the first injection of PBS (A through C), or hMSC-NPs (E through G). Representative GFAP staining from (D), PBS and (H) MSC-NP-injected mice. Endogenous nestin and GFAP expression was determined by immunofluorescence with anti-Nestin or anti-GFAP; transplanted MSC-NPs were detected by DiI red fluorescence, and nuclei detected by DAPI. Sections shows are representative of Group 1 (PBS) in panels A through D, and Group 5 (1×10^6 MSC-NPs $3 \times$) in panels E through H. All samples were visualized by confocal microscopy at 20 \times . Scale bar equivalent to 50 μ m. (I) Graph showing the average number of discrete Nestin positive sites in mice from each group. Values represent mean \pm SE, * $p < 0.05$; ** $p < 0.01$.

MSC-NPs administered intrathecaly. Whether the effects of MSC-NPs seen in EAE pertaining to disease pathology, immunomodulation, and host progenitor cell response will be seen in patients in MS remains to be established. Supplementary materials related to this article can be found online at doi:10.1016/j.jnns.2011.08.036.

Disclosure statement

No competing financial interests exist for any of the authors.

Acknowledgments

We thank Helena Chang from the Department of Biostatistics at Columbia University for assistance with statistical analysis. This work was supported by the Daniel Foundation.

References

[1] Sadg S. Multiple Sclerosis. In: Boland L, editor. *Meritt's neurology*. 11 ed. Philadelphia: Lippincott, Williams, and Wilkins; 2005. p. 941-63.

[2] Hermann A, Caid R, Linde S, Popa MD, Fiedler J, Boehm BO, et al. Efficient generation of neural stem cell-like cells from adult human bone marrow stromal cells. *J Cell Sci* 2004 Sep 1;117(Pt 19):4411-22.

[3] Marcehi R, Nowak M, Buschcinski D, Ferrero L, Guido D, Carbone E, et al. Neural differentiation of human mesenchymal stem cells: evidence for expression of neural markers and eeg K+ channel types. *Exp Neurol* 2005 Nov;24(11):1563-72.

[4] Anjos-Afonso F, Bonnet D, Boulton, culture, and differentiation potential of mouse marrow stromal cells. *Curr Protoc Stem Cell Biol* 2008 Oct;7:2B.3.11-2B.3.11.

[5] Weaver A, Goncalves da Silva A, Nairal RK, Edwards DR, Shapiro SD, Kwon S, et al. An elevated matrix metalloproteinase (MMP) in an animal model of multiple sclerosis. *Nat Protoc* 2006;1(4):1810-9.

[6] Stromer JM, Goveas JM. Active induction of experimental allergic encephalomyelitis. *Nat Protoc* 2006;1(4):1810-9.

[7] Habich A, et al. Intrathecal application of neuroectodermally converted stem cells into a mouse model of ALS: limited intraparenchymal migration. Please cite this article as: Harris VK, et al. Clinical and pathological effects of intrathecal injection of mesenchymal stem cell-derived neural progenitors in an experimental model of multiple sclerosis. *J Neurol Sci* (2011), doi:10.1016/j.jnns.2011.08.036

- and survival narrows therapeutic effects. *J Neural Transm* 2007;114(11):1395–406.
- [8] Janowski M, Kuzma-Kozakiewicz M, Binder D, Habisch HJ, Habisch A, Lukomska B, et al. Neurotransplantation in mice: the concordance-like position ensures minimal cell leakage and widespread distribution of cells transplanted into the cisterna magna. *Neurosci Lett* 2008 Jan 10;430(2):169–74.
- [9] Papadopoulos D, Pham-Dinh D, Reynolds R. Axon loss is responsible for chronic neurological deficit following inflammatory demyelination in the rat. *Exp Neurol* 2006 Feb;197(2):373–85.
- [10] Dominici M, Le Blanc K, Mueller I, Slaper-Cortenbach I, Marini F, Krause D, et al. Minimal criteria for defining multipotent mesenchymal stromal cells. The International Society for Cellular Therapy position statement. *Cytotherapy* 2006;8(4):315–7.
- [11] Di Nicola M, Carlo-Stella C, Magni M, Milanesi M, Longoni PD, Matteucci P, et al. Human bone marrow stromal cells suppress T-lymphocyte proliferation induced by cellular or nonspecific mitogenic stimuli. *Blood* 2002 May 15;99(10):3838–43.
- [12] Gilyarov AV. Nestin in central nervous system cells. *Neurosci Behav Physiol* 2008 Feb;38(2):165–9.
- [13] Xu R, Wu C, Tao Y, Yi J, Yang Y, Zhang X, et al. Nestin-positive cells in the spinal cord: a potential source of neural stem cells. *Int J Dev Neurosci* 2008 Nov;26(7):813–20.
- [14] Nakamura T, Xi C, Hua Y, Hoff JT, Keep RF. Nestin expression after experimental intracerebral hemorrhage. *Brain Res* 2003 Aug 15;981(1–2):108–17.
- [15] Freedman MS. Long-term follow-up of clinical trials of multiple sclerosis therapies. *Neurology* Jan 4 2011;76(1 Suppl 1):S26–34.
- [16] Bates D. Treatment effects of immunomodulatory therapies at different stages of multiple sclerosis in short-term trials. *Neurology* Jan 4 2011;76(1 Suppl 1):S14–25.
- [17] Taveggia C, Feltri ML, Wrabetz L. Signals to promote myelin formation and repair. *Nat Rev Neurol* 2010 May;6(5):276–87.
- [18] Vestereinen HM, Sena ES, French-Constant C, Williams A, Chandran S, Macleod MR. Improving the translational hit of experimental treatments in multiple sclerosis. *Mult Scler* 2010 Sep;16(9):1044–55.
- [19] Fu L, Zhu L, Huang Y, Lee TD, Forman SJ, Shih CC. Derivation of neural stem cells from mesenchymal stem cells: evidence for a bipotential stem cell population. *Stem Cells Dev* 2008 Dec;17(6):1109–21.
- [20] Habisch HJ, Liebau S, Lenk T, Ludolph AC, Brenner R, Storch A. Neuroectodermally converted human mesenchymal stromal cells provide cytoprotective effects on neural stem cells and inhibit their glial differentiation. *Cytotherapy* 2010 Jul;12(4):491–504.
- [21] Delorme B, Ringe J, Pontikoglou C, Gaillard J, Langonne A, Senebe L, et al. Specific lineage-priming of bone marrow mesenchymal stem cells provides the molecular framework for their plasticity. *Stem Cells* 2009 May;27(5):1142–51.
- [22] Russell KC, Phinney DG, Lacey MR, Barrilleaux BL, Meyerholdt KE, O'Connor KC. In vitro high-capacity assay to quantify the clonal heterogeneity in trilineage potential of mesenchymal stem cells reveals a complex hierarchy of lineage commitment. *Stem Cells* 2010 Apr;28(4):788–98.
- [23] Breitbach M, Bostani T, Roell W, Xia Y, Dewald O, Nygren JM, et al. Potential risks of bone marrow cell transplantation into infarcted hearts. *Blood* 2007 Aug 15;110(4):1362–9.
- [24] Zhang C, Zhou C, Teng J, Zhao RL, Song YQ. Multiple administrations of human marrow stromal cells through cerebrospinal fluid pooling survival in a transgenic mouse model of amyotrophic lateral sclerosis. *Cytotherapy* 2009;11(3):299–306.
- [25] Shibuya S, Miyamoto O, Auer RN, Itano T, Mori S, Norimatsu H. Embryonic intermediate filament, nestin, expression following traumatic spinal cord injury in adult rats. *Neuroscience* 2002;114(4):905–16.
- [26] Calza L, Fernandez M, Giuliani A, Aloe L, Giardino L. Thyroid hormone activates oligodendrocyte precursors and increases a myelin-forming protein and NGF content in the spinal cord during experimental allergic encephalomyelitis. *Proc Natl Acad Sci USA* 2002 Mar 5;99(5):3258–63.
- [27] Shin TK, Lee YD, Sim KB. Embryonic intermediate filaments, nestin and vimentin, expression in the spinal cords of rats with experimental autoimmune encephalomyelitis. *J Vet Sci* 2003 Apr;4(1):9–13.
- [28] Duggal N, Schmidt-Kastner R, Hakim AM. Nestin expression in reactive astrocytes following focal cerebral ischemia in rats. *Brain Res* 1997 Sep 12;768(1–2):1–9.
- [29] Bai L, Lennon DP, Eaton V, Maier K, Caplan AL, Miller SD, et al. Human bone marrow-derived mesenchymal stem cells induce Th2-polarized immune response and promote endogenous repair in animal models of multiple sclerosis. *Glia* 2009 Aug 15;57(11):1192–203.
- [30] Gordon D, Pavlovskaya G, Uney JB, Wraith DC, Scolding NJ. Human mesenchymal stem cells infiltrate the spinal cord, reduce demyelination, and localize to white matter lesions in experimental autoimmune encephalomyelitis. *J Neuropathol Exp Neurol* 2010 Oct 11;69(11):1087–95.
- [31] Kassis I, Grigoriadis N, Gowda-Kurkalli B, Mizrachi-Kol R, Ben-Hur T, Slavin S, et al. Neuroprotection and immunomodulation with mesenchymal stem cells in chronic experimental autoimmune encephalomyelitis. *Arch Neurol* 2008 Jun;65(6):753–61.
- [32] Yang J, Yan Y, Cirk B, Yu S, Guan Y, Xu H, et al. Evaluation of bone marrow- and brain-derived neural stem cells in therapy of central nervous system autoimmunity. *Am J Pathol* 2010 Oct;177(4):1989–2001.
- [33] Grigoriadis N, Lourbopoulos A, Lagoudaki R, Frischer JM, Polyzoidou E, Touloumi O, et al. Variable behavior and complications of autologous bone marrow mesenchymal stem cells transplanted in experimental autoimmune encephalomyelitis. *Exp Neurol* 2011 July;230(1):78–89.
- [34] Karussis D, Karageorgiou C, Vaknin-Dembinsky A, Gowda-Kurkalli B, Gornoni JM, Kassis I, et al. Safety and immunological effects of mesenchymal stem cell transplantation in patients with multiple sclerosis and amyotrophic lateral sclerosis. *Arch Neurol* 2010 Oct;67(10):1187–94.
- [35] Mohyeddin Bonab M, Yazdanzadeh S, Lotfi J, Alimoghaddom K, Talebian F, Hooshmand F, et al. Does mesenchymal stem cell therapy help multiple sclerosis patients? Report of a pilot study. *Iran J Immunol* Mar 2007;4(1):50–7.
- [36] Yamout B, Hourani R, Salti H, Barada W, El-Hajj T, Al-Kutoubi A, et al. Bone marrow mesenchymal stem cell transplantation in patients with multiple sclerosis: a pilot study. *J Neuroimmunol* Oct 8 2010;227(1–2):185–9.